

# PA-Efficiency-Aware Hybrid PAPR Reduction for F-OFDM Systems with ICA Based Blind Equalization

Han Lin\*, Xu Zhu<sup>†</sup>, Yufei Jiang\*, Yujie Liu<sup>†‡</sup>, Yuan Zhuang<sup>†</sup> and Lin Gao\*

\* School of Electronic and Information Engineering, Harbin Institute of Technology (ShenZhen), Shenzhen, China

<sup>†</sup> Department of Electrical Engineering and Electronics, The University of Liverpool, Liverpool, UK

<sup>‡</sup> Department of Electrical and Electronic Engineering, Xi'an Jiaotong-Liverpool University, Suzhou, China  
Emails: linhan@stu.hit.edu.cn, {xuzhu,yujieliu,sgyzhua2}@liverpool.ac.uk, {jiangyufei,gaol}@hit.edu.cn

**Abstract**—Filtered-orthogonal frequency division multiplexing (F-OFDM) is a promising candidate waveform for the fifth generation (5G) wireless communications because of its high flexibility and low out-of-band emission (OOBE). However, it suffers from dramatic peak-to-average-power ratio (PAPR), which is higher than that of OFDM and results in the power amplifier (PA) not working in the high-efficiency region. We propose a hybrid PAPR reduction scheme including precoding, time-domain selected mapping (TSLM) and companding techniques, for F-OFDM systems with independent component analysis (ICA) based blind channel equalization, which can achieve significant PAPR reduction over the previous work. Also, this is the first work to reduce PAPR while enabling the PA to work with the highest possible efficiency. The reciprocal of the hybrid PAPR reduction is embedded in the ambiguity elimination process of ICA, and therefore does not require any dedicated side information from the transmitter or any exclusive signal processing at the receiver, leading to a much higher spectral efficiency (SE) and lower computational complexity than the previous work. The bit error rate (BER) performance of the system with the proposed hybrid PAPR reduction scheme is shown to be close to the ideal case with perfect channel state information (CSI), while no side information and training sequence are required for PAPR reduction and channel estimation, thanks to the effectiveness of the ICA based blind channel equalization.

**Index Terms**—Filtered-orthogonal frequency division multiplexing (F-OFDM), peak-to-average-power ratio (PAPR), power amplifier (PA), independent component analysis (ICA).

## I. INTRODUCTION

Filtered-orthogonal frequency division multiplexing (F-OFDM) [1] has been considered as a potential alternative waveform to OFDM [2] in the fifth generation (5G) wireless communications [3], with the following advantages. Firstly, the system parameters can be set with high flexibility. F-OFDM system divides the assigned bandwidth into several unequal-sized sub-bands, and different communication needs are accommodated in different sub-bands with the most

This work was supported in part by the “Liverpool 5G” Project, Department for Digital, Culture, Media and Sport (DCMS), UK, the Science and Technology Innovation Commission of ShenZhen under Project No. J-CYJ20170307151258279 and the Natural Science Foundation of Guangdong Province under grant No. 2018A030313344.

appropriate waveform parameters. Secondly, F-OFDM can reduce the out-of-band emission (OOBE) by using a finite impulse response (FIR) filter in each sub-band and save the bandwidth of guard band with the affordable system complexity. Thirdly, F-OFDM can use the non-contiguous spectral to improve the spectral efficiency (SE).

High peak-to-average-power ratio (PAPR) is a common drawback of multicarrier modulation, which causes signal distortion due to nonlinearity of the power amplifier (PA) and also makes it likely for PA to operate with low efficiency. With  $N$  subcarriers and filters of length  $L_f$ , the PAPR of F-OFDM signals is about  $\frac{L_f+1}{N}$  times higher than that of the conventional OFDM signals [4]. PAPR reduction has been widely investigated for OFDM systems [5]. The companding technique was presented in [6], which reduced PAPR by compressing the signal with a high-amplitude while expanding the signal with a low-amplitude simultaneously. Nevertheless, the spectral regrowth was introduced, resulting in adjacent-channel interference (ACI) and poor bit-error-rate (BER) performance. Selected mapping (SLM) and partial transmit sequence (PTS) are two effective PAPR reduction techniques in [7], which however suffer from high computational complexity due to multiple implementations of inverse discrete Fourier transform (IDFT). This problem could be addressed by the method in [8], which however requires the transmission of side information, and reduces the SE. In [9], an extended SLM (ESLM) algorithm was proposed to resolve the phase ambiguity introduced by SLM without requiring any side information, however, it requires a high computational complexity. The aforementioned PAPR reduction approaches for OFDM systems may not be effective in F-OFDM systems and also did not consider the practical issue of PA efficiency. The PAPR reduction for F-OFDM systems is still an open issue in the literature, which serves the motivation for this work.

Channel estimation and equalization is an essential part for F-OFDM systems. Independent component analysis (ICA) is an effective higher order statistics (HOS) based blind source separation approach that has been used for blind channel estimation and equalization. However, ICA based blind e-

qualization generates phase ambiguity errors at the receiver. In [9], precoding was used to eliminate the ambiguity by introducing the correlation between the source signal and the reference signal.

In this paper, we propose a hybrid PAPR reduction scheme which includes linear precoding, time-domain SLM (TSLM) and companding techniques, for F-OFDM systems with ICA based blind equalization. Our work is different in the following aspects.

- 1) The proposed three-step PAPR reduction scheme outperforms the previous PAPR reduction methods [6] [8] [9]. Also, to the best of our knowledge, this is the first work to consider the practical issue of PA efficiency in PAPR reduction for F-OFDM systems. In light of the fact that the PA efficiency generally increases with the input signal power, we reduce the PAPR while maintaining the signal power as close to the PA saturation point as possible by companding, to enable the PA to work with the highest possible efficiency. While the previous work [5] was only aimed to reduce PAPR as much as possible, which could result in the PA working in a low-efficiency region.
- 2) The reciprocal of the PAPR reduction at the receiver is embedded in the ambiguity elimination process of the ICA based blind channel equalization, and therefore does not require any dedicated side information from the transmitter or any exclusive signal processing at the receiver. Also, the proposed TSLM algorithm operates in time domain with a phase rotation matrix designed off-line and requires less complexity than ESLM [9] without multiple IDFT operations needed. Hence, a much higher SE and a much lower computational complexity are achieved by the proposed hybrid PAPR scheme, compared to the SLM [8] and ESLM [9] approaches.
- 3) The proposed hybrid PAPR reduction scheme does not affect the BER. And the BER performance is shown to be close to the ideal case with perfect channel state information (CSI), with no side information and training sequence required, thanks to the effectiveness of the ICA based blind channel equalization, which is applied to F-OFDM systems for the first time.

The rest of this paper is organized as follows. System model is presented in Section II. The proposed three-step hybrid PAPR reduction scheme and ICA based blind equalization are described in Sections III and IV respectively. Simulation results are given in Section IV. Section VI draws conclusion.

*Notations:* Bold symbols represent matrices or vectors. \* and  $\otimes$  denote linear and circular convolution respectively.  $\text{diag}\{\mathbf{a}\}$  is diagonal matrix with vector  $\mathbf{a}$  on its diagonal.  $\mathbb{E}\{\cdot\}$  is the expectation operator while  $\text{sign}(\cdot)$  is the sign function.

## II. SYSTEM MODEL

For F-OFDM systems, the assigned bandwidth is divided into several unequal-sized sub-bands at the transmitter, and optimal parameters are configured for each sub-band, as shown in Fig. 1 (a). We assume the system has  $N$  subcarriers in one sub-band. We divide a symbol block of length  $L_b$  into  $L_s$  sub-blocks and apply TSLM to each sub-block with  $M = \frac{L_b}{L_s}$  symbols. Let  $d(n, m, k)$  denote the modulated signal on the  $n$ -th ( $n = 0, 1, \dots, N - 1$ ) subcarrier in the  $m$ -th ( $m = 0, 1, \dots, M - 1$ ) symbol of the  $k$ -th ( $k = 0, 1, \dots, L_s - 1$ ) sub-block. To eliminate the ambiguity, a non-redundant linear precoding [9] is employed.

$$X(n, m, k) = \frac{1}{\sqrt{1+a^2}} [d(n, m, k) + a \cdot d_{\text{ref}}(n, m)], \quad (1)$$

where  $d_{\text{ref}}(n, m)$  is the reference signal known to both the transmitter and receiver, and the real number  $a$  ( $0 \leq a \leq 1$ ) is a precoding constant to give a tradeoff of transmit power allocation between the source signal and the reference signal. After precoding, each symbol at the  $N$ -point IDFT can be expressed as

$$x(i_t, m, k) = \frac{1}{\sqrt{N}} \sum_{n=0}^{N-1} X(n, m, k) e^{j \frac{2\pi n i_t}{N}}, \quad (2)$$

where  $i_t = 0, 1, \dots, N - 1$ . Then three-step hybrid PAPR reduction scheme is applied to reduce PAPR and improve PA efficiency, which will be discussed in Section III. A cyclic prefix (CP) of length  $L_{\text{cp}}$  is prepended to each symbol to avoid inter-symbol interference (ISI). Each sub-band needs to pass through an FIR filter. We define the filter impulse response as  $\omega(i_f)$  with length  $L_f$ . Therefore, the output signal of the filter can be given by

$$y(i_o, m, k) = x(i_{\text{cp}}, m, k) * \omega(i_f), \quad i_o \in [0, L - 1], \quad (3)$$

where  $i_{\text{cp}} = 0, 1, \dots, N + L_{\text{cp}} - 1$  and  $i_f = 0, 1, \dots, L_f - 1$ . The transmitted signal sample has a length of  $L = N + L_{\text{cp}} + L_f - 1$ . The channel is assumed to follow quasi-static Rayleigh fading and remain constant within a symbol block. The channel impulse response is defined by  $h(i_h)$  with  $L_h$  taps and  $i_h = 0, 1, \dots, L_h - 1$ . Then, the received signal can be written as

$$r_h(i_o, m, k) = y(i_o, m, k) \otimes h(i_h) + n(i_o, m, k), \quad (4)$$

where  $n(i_o, m, k)$  is the additive white Gaussian noise. The receiver for one sub-band is illustrated in Fig. 1 (b).

## III. HYBRID PAPR REDUCTION SCHEME

We propose a hybrid PAPR reduction scheme for each sub-band of F-OFDM, which consists of three-stages: a) PAPR is first reduced by minimizing the peak power of the reference signal through precoding coefficient, b) a low-complexity TSLM scheme is proposed to reduce PAPR, whose phase ambiguity is eliminated with ICA-induced ambiguities without

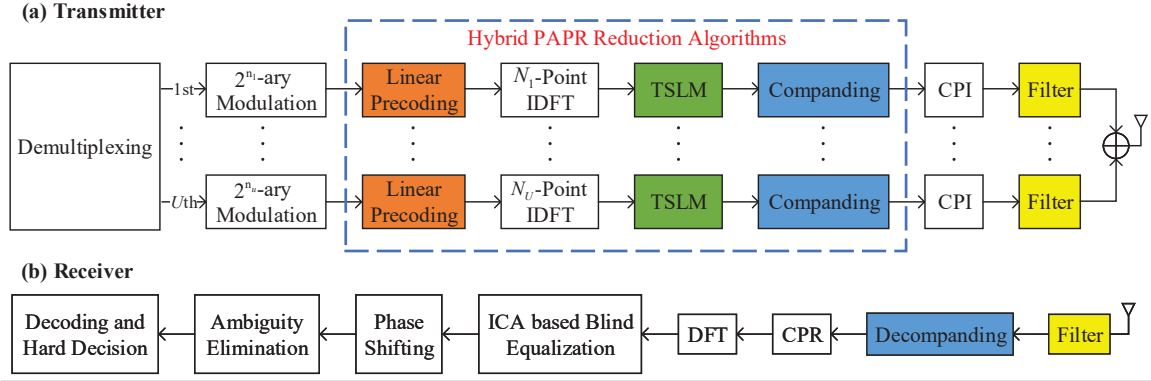


Fig. 1. (a) Transmitter of F-OFDM with  $U$  sub-bands, (b) Receiver of F-OFDM. (CPI:cyclic prefix insertion, CPR:cyclic prefix removal)

requiring any side information and c) the comanding with consideration of PA efficiency is implemented last, which not only further reduces PAPR but also enables the PA to operate in high-efficiency region.

#### A. Linear Precoding

Linear precoding can be designed through two aspects: a) reference signal design  $d_{\text{ref}}(n, m)$  and PAPR reduction coefficient  $c(n, m)$ . Reference signal is designed off-line to jointly eliminate the ambiguities induced by the proposed hybrid PAPR reduction scheme and ICA based blind equalization. Hadamard matrix in [10] is utilized for the reference signal design. A Hadamard matrix  $\mathbf{H}_M$  of size  $M \times M$  is a square orthogonal matrix and each row has  $\frac{M}{2}$  1's and  $\frac{M}{2}$  -1's except the first row. One row within the second to the  $M$ -th row of  $\mathbf{H}_M$  is randomly selected as the reference signal for  $n$ -th subcarrier of  $M$  symbols in the  $k$ -th sub-block.

$$d_{\text{ref}}(n, m) = c(n, m)\mathbf{H}_M^n(i_n, m), \quad 2 \leq i_n \leq M, \quad (5)$$

where  $c(n, m)$  is a real number to minimize the peak power of precoded signal. Pseudo noise (PN) sequence is designed for  $c(n, m)$  to reduce the PAPR [9].

#### B. Time-Domain Selected Mapping

The existing SLM scheme in [7] demonstrates a good PAPR reduction performance. However, it has two drawbacks a) high training overhead due to the transmission of side information and b) high computational complexity resulting from multiple IDFT implementations on F-OFDM signal candidates. To tackle these problems, a time-domain SLM PAPR reduction scheme is proposed, where its phase ambiguity is eliminated together with ICA-induced ambiguities by performing correlation between the received signal and reference signal without requiring any side information and its PAPR reduction is performed in time-domain requiring one IDFT operation only with a significant complexity reduction over the existing method [9].

In conventional SLM [7],  $S$  independent candidate signals can be generated by  $S$  phase rotation sequences multiplied by a symbol  $\mathbf{X}$  consisting of  $N$  subcarriers in the frequency domain.

$$\mathbf{X} = [X_0, X_1, \dots, X_{N-1}]^T, \quad (6)$$

The phase rotation sequence matrix can be expressed as

$$\mathbf{F}_i = \text{diag} [f_0^i, f_1^i, \dots, f_{N-1}^i], \quad (7)$$

where  $i$  ( $i = 0, 1, \dots, S - 1$ ) denotes the index of phase rotation factor  $f_n^i \in \{\pm 1, \pm j\}$ . Then, the candidate signal can be obtained as

$$\mathbf{S}_i = \mathbf{F}_i \mathbf{X} = [f_0^i X_0, f_1^i X_1, \dots, f_{N-1}^i X_{N-1}]^T. \quad (8)$$

Each candidate symbol  $\mathbf{S}_i$  requires IDFT operation,

$$\mathbf{s}_i = \mathbf{D}^{-1} \mathbf{S}_i, \quad (9)$$

where  $\mathbf{D}$  is the DFT matrix. Therefore, multiple IDFT operations are required for each candidate symbol.

To reduce the complexity, the phase rotation matrix denoted by  $\mathbf{T}_i$  ( $i = 0, 1, \dots, S - 1$ ) in the time domain can be developed to replace the IDFT operations in the previous SLM technique [8].

$$\mathbf{s}_i = \mathbf{T}_i \mathbf{x}, \quad (10)$$

where  $\mathbf{x} = \mathbf{D}^{-1} \mathbf{X}$ . According (7) to (11), we obtain

$$\mathbf{s}_i = \mathbf{D}^{-1} \mathbf{F}_i \mathbf{D} \mathbf{x}. \quad (11)$$

Therefore, the phase conversion matrix can be obtained as

$$\mathbf{T}_i = \mathbf{D}^{-1} \mathbf{F}_i \mathbf{D}. \quad (12)$$

The computational complexity of TSLM for a sub-block of  $M$  symbols is shown in Table I. It can be easily observed that the proposed TSLM has a much lower computational complexity than the existing methods in [7] and [9].

TABLE I: Complexity Analysis

PAPR Reduction Methods	Number of Multiplication
Conventional SLM [7]	$SM \cdot N \log_2 N$
ESLM [9]	$SM \cdot N \log_2 N$
TSLM	$SM \cdot 3N$

The phase ambiguity introduced by TSLM will be eliminated with ambiguities of ICA by the well-designed reference signal in Section IV, with no side information and training sequence. The procedure of TSLM can be described in detail for each sub-block as shown in Algorithm. 1. The steps 2 and 3 can be designed off-line.

---

**Algorithm 1** Time-Domain SLM Algorithm (TSLM)
 

---

**Input:** Initialize  $S$  and  $iter = 1$ .

- 1: **Begin**
  - 2: Generate  $S$  phase rotation sequences,  $i = 0, 1, \dots, S-1$ .  
 $\mathbf{F}_i = \text{diag}[f_0^i, f_1^i, \dots, f_{N-1}^i]$ ,  $f_n^i \in \{\pm 1, \pm j\}$ .
  - 3: Calculate  $S$  phase rotation matrices in time domain  
 $\mathbf{T}_i = \mathbf{D}^{-1} \mathbf{F}_i \mathbf{D}$ ,  $i = 0, 1, \dots, S-1$ .
  - 4: **while**  $iter \leq S$  **do**
  - 5:  $i = iter - 1$
  - 6: **for**  $m = 0, 1, \dots, M-1$  **do**
  - 7:  $\mathbf{s}_i(m) = \mathbf{T}_i \cdot \mathbf{x}(m)$
  - 8:  $\text{PAPR}\{\mathbf{s}_i(m)\} = \frac{\max_{0 \leq n \leq N-1} |s_i(n, m)|^2}{\mathbb{E}[|s_i(n, m)|^2]}$
  - 9: **end for**
  - 10: Find maximum PAPR:  
 $\text{PAPR}_{\max}^i = \max_{0 \leq m \leq M-1} \{\text{PAPR}\{\mathbf{s}_i(m)\}\}$
  - 11:  $iter = iter + 1$ .
  - 12: **end while**
  - 13:  $\mathbf{T}_{\text{opt}} = \arg \min_{0 \leq i \leq S-1} \{\text{PAPR}_{\max}^i\}$
  - 14: **End**
- Output:** Optimal phase rotation matrix  $\mathbf{T}_{\text{opt}}$ .
- 

### C. Companding

At the transmitter, the  $\mu$ -law companding technique with the consideration of PA efficiency is proposed to perform on each F-OFDM symbol, which can not only further reduce PAPR greatly but also allow high PA efficiency. Denote  $s_i(n, m, k)$  ( $i \in [0, S-1]$ ) as the symbol selected by TSLM, and after companding we can obtain

$$s_c(n, m, k) = \frac{A \ln(1 + \mu | \frac{s_i(n, m, k)}{A} |)}{\ln(1 + \mu)} \cdot \text{sign}(s_i(n, m, k)), \quad (13)$$

where  $\mu$  ( $\mu > 0$ ) is the companding factor and  $A$  is specified to be smaller than the saturation point of PA. It is noteworthy that PAPR can be reduced significantly by selecting a larger  $\mu$ . However, a large  $\mu$  is likely to degrade the BER performance due to the signal distortion. Hence, there should be a trade-off performance between PAPR

reduction and BER performance. Moreover, by choosing a larger  $A$ , the signal power is much closer to the saturation point so that the PA can work with high efficiency and the PAPR is reduced greatly owing to the increased averaged signal power. Hence, the proposed PA-efficiency-awareness companding technique can not only reduce PAPR greatly but also enhance the PA efficiency significantly. Due to the introduction of spectral regrowth the companding technique would suffer from ACI and degrade BER performance in OFDM systems, which however are avoided in the proposed F-OFDM systems thanks to the utilization of FIR filters.

After decompanding at the receiver, we obtain

$$r_d(n, m, k) = \frac{A}{\mu} \left( e^{\frac{|r(n, m, k)| \ln(1 + \mu)}{A}} - 1 \right) \quad (14)$$

### IV. ICA BASED BLIND EQUALIZATION

ICA based blind equalization is exploited to recover the transmitted signal after decompanding, CP removal and DFT implementation of the received signal at the receiver, by performing correlation between the received signal and the well-designed reference signal.

First, received signal  $r_d(n, m, k)$  is whitened [11] by principal component analysis (PCA) [12] and the whitening coefficient on the  $n$ -th subcarrier is denoted by  $C_w(n)$ . Then JADE [13] is applied on a symbol block of length  $L_b$  to obtain equalization coefficient  $J_{\text{ICA}}(n)$ .

$$\hat{r}(n, m, k) = J_{\text{ICA}}(n) \cdot C_w(n) \cdot r_d(n, m, k). \quad (15)$$

Phase ambiguity exists in the ICA equalized signal  $\hat{r}(n, m, k)$  even in the absence of noise, which can be resolved by the de-rotation operation as

$$\check{r}(n, m, k) = \hat{r}(n, m, k) \cdot \frac{\alpha(n)}{|\alpha(n)|}, \quad (16)$$

where  $\alpha(n)$  is used to correct the phase deviation [12].

$$\alpha(n) = \left\{ \frac{1}{L_b} \sum_{k=0}^{L_b-1} \sum_{m=0}^{M-1} [\hat{r}(n, m, k)]^4 \right\}^{-\frac{1}{4}} e^{j \frac{\pi}{4}} \quad (17)$$

$$\approx g(n) e^{j \frac{\pi}{2} l} \quad (l \in \{0, 1, 2, 3\}).$$

Although phase ambiguity can be resolved by phase shifting in (16), it introduces quadrant ambiguity in  $\check{r}(n, m, k)$ . The estimated symbols after quadrant ambiguity elimination can be obtained as

$$\tilde{r}(n, m, k) = p(n, k) \cdot \check{r}(n, m, k), \quad (18)$$

Assuming perfect phase shifting in (16), the cross correlation  $\rho_{(n, k)}$  between the detected signal and the reference signal on the  $n$ -th subcarrier in the  $k$ -th subblock is written as

$$\rho_{(n, k)} = \frac{1}{M} \sum_{m=0}^{M-1} \{\check{r}(n, m, k) \cdot [d_{\text{ref}}(n, m)]^*\}. \quad (19)$$

Then, the phase shifts introduced by both ICA equalization and TSLM can be obtained as

$$p(n, k) = [e^{-j\frac{\pi}{4}} \cdot \text{sign}(\frac{\rho(n,k)}{|\rho(n,k)|})]^{-1}. \quad (20)$$

Therefore, ambiguities introduced by both PAPR reduction and ICA equalization have been eliminated jointly by the well-designed reference signal and then the transmitted signal can be recovered.

## V. SIMULATION RESULTS

Simulation results are provided to demonstrate the performances of the proposed hybrid PAPR reduction scheme and ICA based blind equalization technique. System parameters are set as follows: each sub-band of F-OFDM systems has  $N = 64$  subcarriers; each symbol block of length  $L_b = 128$  has  $L_s = 4$  sub-blocks each with  $M = 32$  symbols; iteration factor of TSLM of  $S = 8$  is set; QPSK modulation scheme is utilized; the precoding constant is specified as  $a=0.32$ .

### A. PAPR Reduction

Fig. 2 shows the performance of the proposed hybrid PAPR reduction scheme, in comparison to the precoding [9], ESLM [9] and  $\mu$ -law companding [6] approaches, in terms of the complementary cumulative distribution function (CCDF) of PAPR which is defined by  $\text{CCDF} = \text{Probability}(\text{PAPR} \geq \gamma)$  dB. Among the three individual schemes, the precoding based method has the worst performance while the companding enabled scheme performs best. The PAPR reduction performance can be enhanced significantly by the proposed hybrid scheme, with approximately 5.5 dB improvement over original F-OFDM signal at  $\text{CCDF} = 10^{-3}$ .

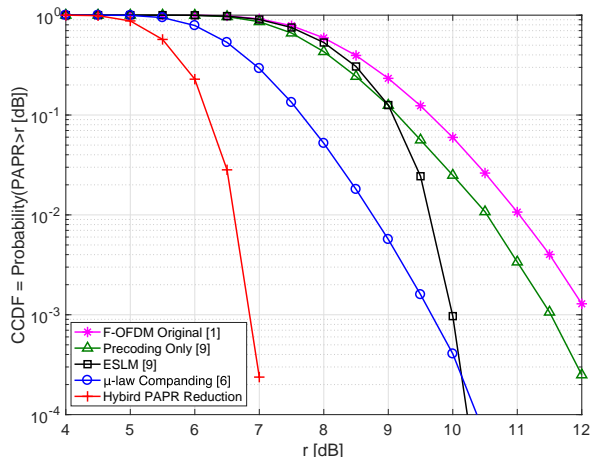


Fig. 2. CCDF performance of PAPR reduction algorithms

Table II illustrates the values of peak power, mean power and PAPR of the proposed hybrid PAPR reduction scheme and the existing ESLM method [9] respectively. It is easily

seen that the proposed hybrid scheme can not only achieve a lower PAPR but also demonstrate higher mean power than the existing ESLM method, which allows the PA to operate in a higher efficiency region. For instance, the mean power of the proposed hybrid scheme can be as large as 15 dBm, which is approximately 5 dBm larger than the existing ESLM. Since the PA of the proposed hybrid scheme operates with a higher power, it allows a much higher efficiency than the existing ESLM method, thanks to the PA-efficiency-awareness of the proposed scheme design.

TABLE II: Resulting power of PA-efficiency aware hybrid PAPR reduction in comparison to ESLM [9]

PAPR Reduction Methods	Peak Power	Mean Power	PAPR
ESLM [9]	19.6 dBm	10.2dBm	9.4dB
Hybrid PAPR Reduction	21.3 dBm	15.0dBm	6.3dB

Fig. 3 demonstrates the impact of the companding factor  $\mu$  on the CCDF performance of the proposed hybrid PAPR reduction scheme. It is easily observed that PAPR is reduced greatly with the increase of  $\mu$ , as discussed in Section III. For example, at  $\text{CCDF} = 10^{-3}$ , PAPR is reduced by the proposed hybrid scheme from 8.1 dB to 6.8 dB as  $\mu$  increases from 2 to 5.

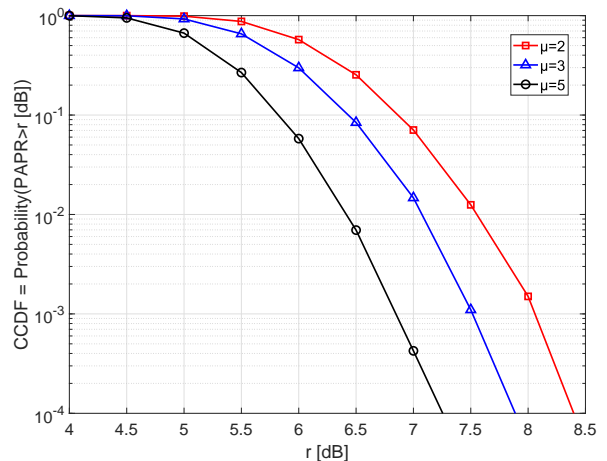


Fig. 3. Impact of companding factor  $\mu$  on PAPR performance of the proposed hybrid scheme

### B. BER Performance

The BER performance of the proposed system with hybrid PAPR reduction and ICA based equalization is shown in Fig. 4, where various values of  $\mu$  are used and zero-forcing (ZF) with perfect CSI and no companding is used as a benchmark. We can observe that the BER performance of the proposed hybrid scheme degrades as  $\mu$  increases. This is because the increase  $\mu$  is likely to enhance the noise power as discussed in Section III. Thanks to the utilization of

blind ICA equalization, the proposed scheme even provides a slightly better BER performance than ZF with perfect CSI information. This is because ZF equalization could enhance the noise power, whereas ICA is an HOS-based method and the fourth or higher order cumulants of Gaussian noise are equal to zero [14].

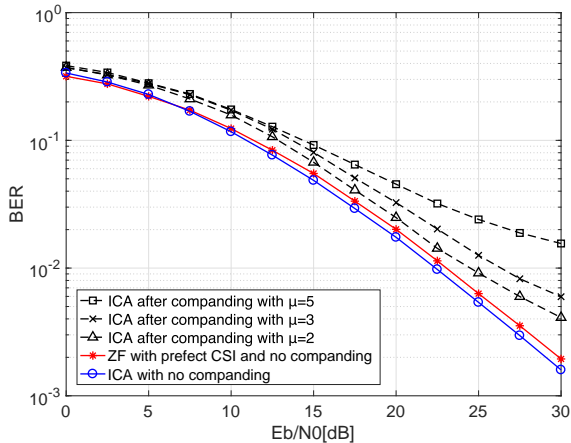


Fig. 4. BER performance with PAPR reduction and ICA blind equalization

### C. OOB E Suppression

Fig. 5 shows the effect of companding on the power spectral density (PSD) of F-OFDM and OFDM systems. After companding with  $\mu = 5$ , OFDM suffers from a spectrum regrowth with 15 dB. However, this problem is avoided in F-OFDM systems, thanks to the ACI mitigation and guard interval reduction. As the companding factor  $\mu$  increases, the OOB E becomes much worse. In contrast, the OOB E can be suppressed by 150 dB in F-OFDM systems regardless of the companding factors.

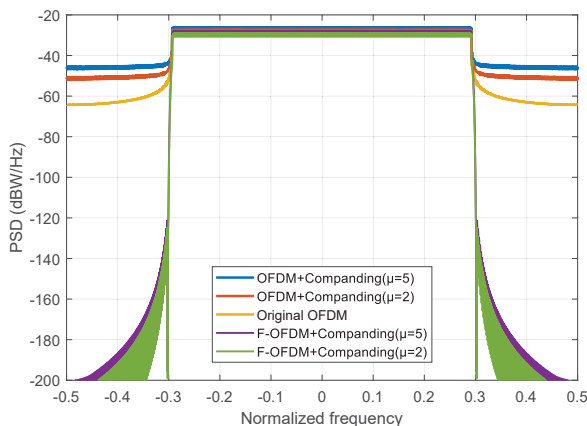


Fig. 5. PSD comparison of companded signal and filtered signal

## VI. CONCLUSIONS

In this paper, we have proposed a hybrid PAPR reduction scheme which consists of non-redundant linear precoding, TSLM and companding. It achieves a significant gain of 5.5 dB over the original F-OFDM signal and also outperforms the previous PAPR reduction approaches in [6], [8] and [9]. The proposed PAPR reduction scheme is PA-efficiency aware, and by maintaining the signal power to as close to the PA saturation point as possible through companding, it enables a higher operating PA efficiency than ESLM [9] does. The ambiguity introduced by PAPR reduction is resolved blindly through the ICA based equalization, and therefore no dedicated side information is required for TSLM, featuring a higher SE than the previous schemes [8]. The BER performance is not affected by PAPR reduction and is close to the case with perfect CSI, thanks to the effectiveness of ICA.

## REFERENCES

- [1] X. Zhang, M. Jia, L. Chen, J. Ma, and J. Qiu, "Filtered-OFDM - Enabler for flexible waveform in the 5th generation cellular networks," in *Proc. IEEE Globecom 2015*, San Diego, CA, USA, Dec. 2015, pp. 1–6.
- [2] T. Hwang, C. Yang, G. Wu, S. Li, and G. Y. Li, "OFDM and its wireless applications: A survey," *IEEE Trans. Veh. Technol.*, vol. 58, no. 4, pp. 1673–1694, May. 2009.
- [3] C. Wang, F. Haider, X. Gao, X. You, Y. Yang, D. Yuan, H. M. Aggoune, H. Haas, S. Fletcher, and E. Hepsaydir, "Cellular architecture and key technologies for 5G wireless communication networks," *IEEE Commun. Mag.*, vol. 52, no. 2, pp. 122–130, Feb. 2014.
- [4] X. Wang, S. Burkert, and S. ten Brink, "On peak to average power ratio of universal filtered OFDM signals," in *Proc. IEEE PIMRC 2017*, Montreal, QC, Canada, Oct. 2017, pp. 1–7.
- [5] Y. Rahmatallah and S. Mohan, "Peak-to-average power ratio reduction in OFDM systems: A survey and taxonomy," *IEEE Commun. Surveys Tutorials*, vol. 15, no. 4, pp. 1567–1592, Nov. 2013.
- [6] N. Ali, R. Almahainy, A. Al-Shabli, N. Almoosa, and R. Abd-Alhameed, "Analysis of improved  $\mu$ -law companding technique for OFDM systems," *IEEE Trans. Consum. Electron.*, vol. 63, no. 2, pp. 126–134, May. 2017.
- [7] D. Lim, S. Heo, and J. No, "An overview of peak-to-average power ratio reduction schemes for OFDM signals," *J. Commun. Netw.*, vol. 11, no. 3, pp. 229–239, Jun. 2009.
- [8] C.-L. Wang and S.-J. Ku, "Novel conversion matrices for simplifying the IFFT computation of an SLM-based PAPR reduction scheme for OFDM systems," *IEEE Trans. Commun.*, vol. 57, no. 7, pp. 1903–1907, Jul. 2009.
- [9] J. Gao, X. Zhu, and A. K. Nandi, "Non-redundant precoding and PAPR reduction in MIMO OFDM systems with ICA based blind equalization," *IEEE Trans. Wireless Commun.*, vol. 8, no. 6, pp. 3038–3049, Jun. 2009.
- [10] S. Georgiou, C. Koukouvinos, and J. Seberry, *Hadamard matrices, orthogonal designs and construction algorithms*. Kluwer Academic Publishers, 2003.
- [11] J. C. Rajapakse, "Adaptive blind signal and image processing: learning algorithms and applications [book review]," *IEEE Trans. Neural Networks*, vol. 14, no. 6, pp. 1580–1580, 2004.
- [12] L. Sarperi, X. Zhu, and A. K. Nandi, "Blind OFDM receiver based on independent component analysis for multiple-input multiple-output systems," *IEEE Trans. Wireless Commun.*, vol. 6, no. 11, pp. 4079–4089, Nov. 2007.
- [13] J. Cardoso, "High-order contrasts for independent component analysis," *Neural Computation*, vol. 11, no. 1, pp. 157–192, Jan. 1999.
- [14] A. Cichocki and S. Amari, *Adaptive Blind Signal and Image Processing*. Chichester, U.K.: Wiley, 2003.